

EMI modeling of switching circuits via augmented equivalents and measured data

Original

EMI modeling of switching circuits via augmented equivalents and measured data / Trinchero, Riccardo; Stievano, IGOR SIMONE; Canavero, Flavio. - STAMPA. - (2015), pp. 130-133. (2015 IEEE International Symposium on Electromagnetic Compatibility (EMC) Dresden (Ge) Aug. 16-22, 2015) [10.1109/IEMC.2015.7256145].

Availability:

This version is available at: 11583/2621706 since: 2016-01-21T11:53:14Z

Publisher:

IEEE

Published

DOI:10.1109/IEMC.2015.7256145

Terms of use:

This article is made available under terms and conditions as specified in the corresponding bibliographic description in the repository

Publisher copyright

(Article begins on next page)

EMI Modeling of Switching Circuits via Augmented Equivalents and Measured Data

Riccardo Trincherio, Igor S. Stievano, Flavio G. Canavero

EMC Group, Department of Electronics and Telecommunications, Politecnico di Torino

Corso Duca degli Abruzzi 24, 10129 Torino, Italy

E-mail: {riccardo.trincherio, igor.stievano, flavio.canavero}@polito.it.

Abstract—This paper presents an innovative modeling technique for the prediction of the conducted emissions generated by switching circuits. The proposed approach accounts for the inherent time-varying nature of the above class of circuits by means of an augmented impedance or admittance one-port representation estimated from real measurements. The above interpretation yields to an improved accuracy with respect to the state-of-the-art modeling approaches based on linear time-invariant surrogates and allows for the full characterization of the conducted disturbances via a well-defined modeling procedure. The strength of the method is verified on a real dc-dc boost converter.

I. INTRODUCTION

Switching circuits are widely used in almost any electrical and electronic equipment and appliances. Without loss of generality, dc-dc power converters, dc motors and inverters are typical examples belonging to this classification that share the common behavior of exhibiting periodically time-varying responses arising from the internal activity of the switching components. Within the EMC framework, the above features yield to discontinuous absorbed currents that behave as noisy disturbances feeding the power distribution network that need to be fully characterized and modeled to comply with the EMC regulations for the conducted emissions (CE) [1].

The common approach to CE prediction is based on the Fourier transform of the steady-state portion of the aforementioned current waveforms obtained via time-domain simulations [2]. The above method is simple, but it requires an intimate knowledge of the device under test and long simulation time to achieve accurate results. A widely adopted alternative is provided by simplified linear time-invariant (LTI) behavioral models obtained from real measurements. Without loss of generality the readers are referred to [3]–[7] for a selection of the state-of-the-art contributions based on Norton- or Thevenin-like equivalents. The main drawback of the latter approaches resides in the possible inaccuracies of the CE predictions for different design configurations of the circuit.

To overcome the above limitation, this paper introduces an alternative frequency-domain modeling approach based on the theory of periodical linear time-varying (PLTV) systems and on the generation of an augmented black-box admittance representation [8]–[11]. The proposed equivalent can be readily estimated from real measurements via a simple extraction procedure. In addition, the aforementioned method explains the mechanism of the generation of EMI disturbances due to

the harmonic coupling introduced by the switching elements of the circuit and the lack of accuracy of simplified LTI models, thus offering a novel approach to electromagnetic interference (EMI) prediction.

II. APPLICATION TEST CASE

The feasibility and the strength of the proposed approach is demonstrated on the example switching converter shown in Fig. 1. It provides a representative test case sharing the same key features of the typical absorbed currents of any switching circuit connected to the supply main.

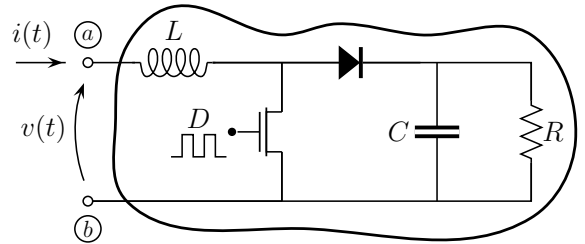


Figure 1. Example dc-dc boost converter used in the paper for illustrating the proposed modeling method.

The converter is designed to operate in continuous mode at a switching frequency $f_c = 50$ kHz, with duty cycle $D = 50\%$ and a nominal input voltage $v = 5$ V. The circuit parameters are: $L = 470 \mu\text{H}$, $C = 470 \mu\text{F}$, $R = 150 \Omega$, the diode model is FES16DT and the n-channel MOS model is IRFU4105.

It is worth remarking that the above example can be seen as a PLTV circuit when the MOS and the diode are approximated by periodic linear switches. The above assumption is the common underlying hypothesis used in many state-of-the-art methods for the prediction of the steady-state behavior of a switching circuit (e.g., see [9], [10]).

III. THEORETICAL FRAMEWORK

This Section briefly introduces the theoretical framework needed to understand and to model the CE of a generic switching circuit, such as the boost converter of Fig. 1. For this example and a constant voltage excitation, e.g., $v(t) = 5$ V, the current $i(t)$ drawn by the power supply turns out to be characterized by a periodic response, as the one of Fig. 2. The above current behavior, that arises from the slicing effects introduced by the time-varying activity of the internal switching elements, unavoidably leads to absorbed currents with a

discrete frequency spectrum. As seen in the bottom panel of Fig. 2, the spectrum is defined by a large number of harmonics located at the integer multiples of the switching frequency f_c .

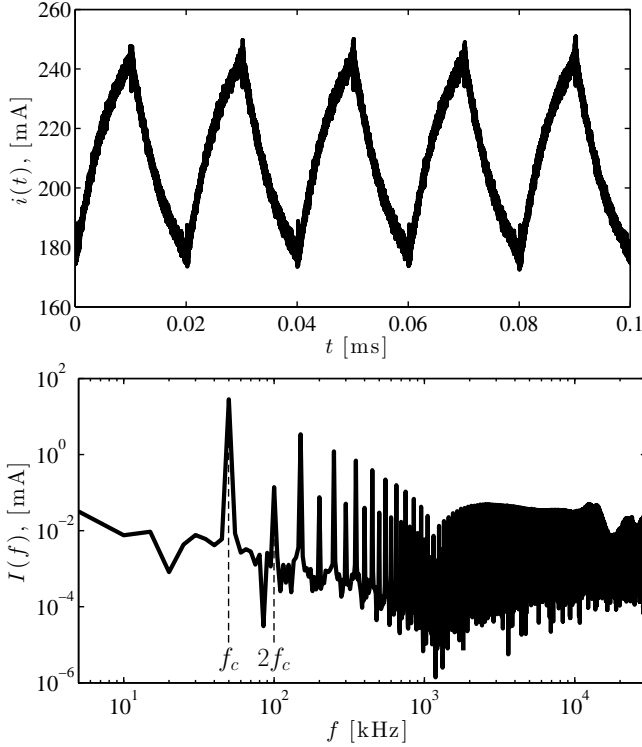


Figure 2. Measured steady-state current response $i(t)$ of the boost example of Fig. 1 (top panel) and its corresponding frequency-domain spectrum $I(f)$ (bottom panel).

The above discussion, along with the theory of time-varying circuits and systems, justify the typical behavior of this class of circuits that are characterized by the generation of new harmonics in their current and voltage responses [8].

This feature also suggests to seek for a suitable relationship in the frequency-domain to model the CE of the boost example of Fig. 1, i.e., to predict the current $i(t)$ as a function of $v(t)$. According to [9]–[11], this is achieved via the following relation:

$$\mathbf{I} \approx \mathbf{YV} \quad (1)$$

where vectors $\mathbf{V} = [V_{-N}, \dots, V_N]^T$ and $\mathbf{I} = [I_{-N}, \dots, I_N]^T$ collect the Fourier coefficients of the corresponding steady-state periodic circuit responses and N is the expansion order that defines the number of positive harmonics used to represent the voltage and current variables.

The above equation, that plays the role of an *augmented* admittance representation, is fully described by a $(2N + 1) \times (2N + 1)$ matrix that writes:

$$\mathbf{Y} = \begin{bmatrix} Y_0(\Omega - N\omega_c) & \dots & \vdots & \dots & \vdots \\ Y_1(\Omega - N\omega_c) & \dots & Y_{-1}(\Omega) & \dots & \vdots \\ Y_2(\Omega - N\omega_c) & \dots & Y_0(\Omega) & \dots & Y_{-2}(\Omega + N\omega_c) \\ \vdots & \dots & Y_1(\Omega) & \dots & Y_{-1}(\Omega + N\omega_c) \\ \vdots & \dots & \vdots & \dots & Y_0(\Omega + N\omega_c) \end{bmatrix}, \quad (2)$$

where the entries $Y_n(\omega)$ are the so-called frequency-domain aliasing admittances, Ω is the angular frequency of the sinusoidal voltage excitation of the circuit (e.g., for a boost converter $\Omega = 0$ rad/s) and $\omega_c = 2\pi f_c$ is the fundamental angular frequency defining the periodic switching activity of the circuit.

It is important to notice that the above equation provides an approximation of the system behavior with a tunable accuracy that depends on the expansion order N . Specifically, the maximum frequency covered by (1) is $f_{max} = Nf_c$. Also, matrix \mathbf{Y} completely characterizes the voltage-current behavior of a two-terminal PLTV element and generalizes the classical concept of LTI admittances. In the latter case, the augmented matrix (2) becomes diagonal since LTI circuit elements do not involve constitutive relations with coupling among the different harmonics of their port voltage and current variables. The above observation explains that a full admittance matrix is therefore needed to take into account the aforementioned coupling arising from the time-varying activity of the circuit.

According to [11], a circuit consisting of the interconnection of a PLTV circuit with standard LTI elements can be suitably simulated in frequency-domain by replacing the whole circuit with an augmented representation of order N . The resulting augmented circuit, which has a total number of nodes that is $(2N + 1)$ times larger than the original network, is generated by circuit inspection and topological rules only. Each node voltage or branch current of the above augmented description represents a single harmonic of the Fourier expansion of the corresponding voltage or current variable. The resulting augmented circuit can be simulated via standard tools for circuit analysis, e.g., modified nodal analysis (MNA), providing the spectrum of the steady-state current and voltage variables up to the maximum frequency f_{max} via a single frequency-domain simulation.

Hence, the above procedure can be effectively applied to predict the behavior of a switching circuit characterized via (2) that is connected to the supply main e.g., via a suitably designed filter, thus allowing to assess systematically the effectiveness of different design strategies for EMI suppression.

IV. MODELING FROM MEASURED DATA

The theoretical framework presented in the previous Section allows to describe a generic PLTV two-terminal element via the augmented admittance (2), that can be filled in by a set of real measurements according to the setup of Fig. 3. In the above setup, the boost converter is connected to a real source defined by the series connection of an ideal voltage generator and of its internal impedance.

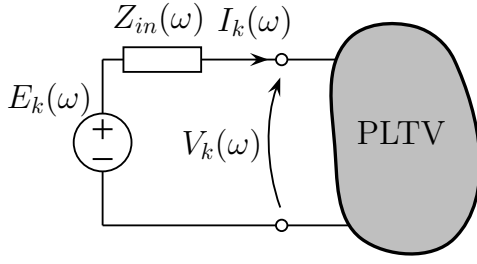


Figure 3. Ideal setup used to illustrate the k -th measurement of the procedure for the estimation of the augmented admittance representation of the PLTV element.

The entries of the admittance matrix can be estimated via a series of measurements of the current $I_k(\omega)$ and the voltage $V_k(\omega)$ responses (see Fig. 3) to a set of voltage excitations $E_k(\omega)$ where $k = 1, \dots, (2N + 1)$ by recasting the equation (1) into the following linear problem.

$$\mathbf{Y} \approx [\mathbf{I}_1, \dots, \mathbf{I}_{2N+1}][\mathbf{V}_1, \dots, \mathbf{V}_{2N+1}]^{-1} \quad (3)$$

where \mathbf{V}_k and \mathbf{I}_k are column vectors that collect the first $(2N + 1)$ harmonics of the voltage $V_k(\omega)$ and current $I_k(\omega)$ spectra sampled at the integer multiples of the switching frequency f_c (e.g., $\mathbf{V}_k = [V_k(-Nf_c), \dots, V_k(Nf_c)]^T$).

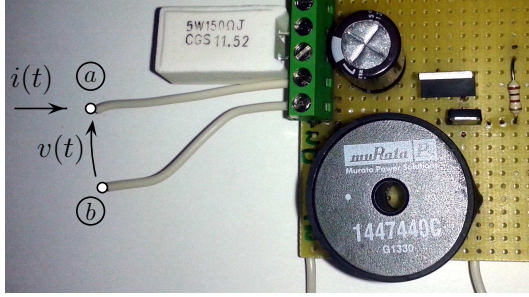


Figure 4. Practical realization of the boost converter of Fig. 1.

The proposed modeling strategy is used to estimate the admittance matrix \mathbf{Y} of the dc-dc converter of Fig. 1. A central angular frequency $\Omega = 0$ is used since the boost operates in an ideal condition with a dc source connected to its input port. Figure 4 shows the test circuit implementing the schematic of Fig. 1 used to collect the real measured data and to validate the proposed modeling methodology. The measurements are performed in time-domain by means of a digital scope (LeCroy 7300A and passive voltage probes) and the corresponding spectra are computed offline via MATLAB and the fast Fourier transform (FFT) routine. The voltage excitations $e_k(t)$ are generated by a function waveform generator (Agilent 33250A).

For practical reasons, the number of current and voltage measurements has to be limited in a range 10–20, yielding to an augmented matrix that covers the low-frequency functional switching activity of the converter only (see Fig. 5). The high-frequency behavior of the PLTV circuit can be predicted and modeled by extending the diagonal part and the central column of the admittance matrix only with the help of an LTI equivalent. The latter equivalent, obtained from measurement data, can be interpreted as a voltage dependent Norton

equivalent. The new order of the augmented matrix can be therefore extended to a much larger value (e.g., $N = 1000$), thus allowing to cover the entire bandwidth required for the CE characterization of this class of circuits, from 150 kHz to 30 MHz.

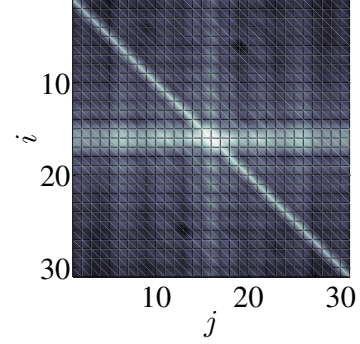


Figure 5. Measured admittance matrix \mathbf{Y} for $N = 15$. The grayscale image provides a graphical information of the absolute values of the matrix entries where white color is used for large dominant relative contributions.

V. RESULTS

In this Section the CE of the boost converter of Fig. 4 are estimated by means of the proposed method and of the classical behavioral Norton-based approach and compared with real measured data. The device under modeling is connected to the supply main through a line impedance stabilization network (LISN) and a series resistance R_s as shown in the schematic of Fig. 6. The resistor R_s has been inserted to change the operating condition of the converter (in the validation test discussed below $R_s = 56 \Omega$).

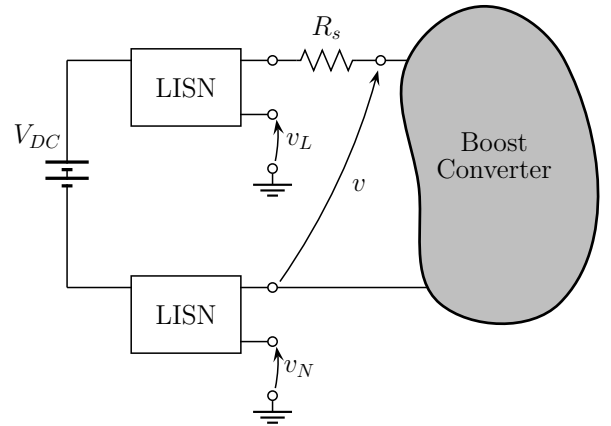


Figure 6. Experimental setup for the simulation and the measurements of the DM emissions of the boost converter introduced in Sec. II.

The differential mode (DM) CE are computed by the following relation:

$$V_{DM}(\omega) = \frac{V_L(\omega) - V_N(\omega)}{2} \quad (4)$$

The measurement setup is simulated as outlined in Sec. III (see [9]–[11] for additional details) without considering the parasitic elements of the LISN and without modeling the electrical path of the common mode noise.

Figure 7 collects both the time-domain response of the differential mode voltage $v_{DM}(t)$ and its corresponding spectrum and compares measured data with the predictions obtained via the two approaches considered in the study. This test highlights the inaccuracies of the simplified LTI models and confirms the improved accuracy of the proposed approach, that turns out to provide a full characterization of the behavior of a PLTV circuit and offers a weak dependence on the operating condition. On the contrary, the curves in the figure highlight the unavoidable lack of accuracy of simplified LTI models as these based on Norton-like elements.

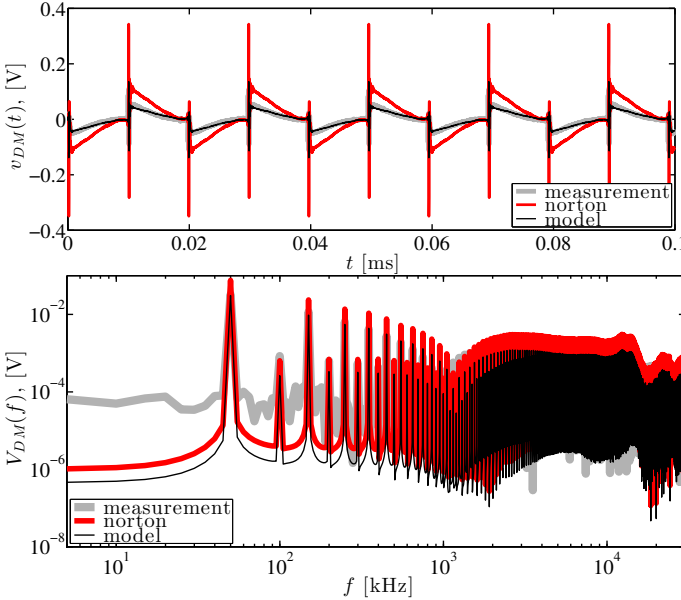


Figure 7. DM noise voltage response of the validation test case shown in Fig. 6 ($R_s = 56 \Omega$). Light gray curves: measurement; red curves: Norton-based prediction; black curves: proposed method.

VI. CONCLUSIONS

This paper addressed the behavioral modeling of the CE generated by a switched circuit, that is considered as a two-terminal PLTV element characterized by means of an augmented admittance representation. The augmented admittance is estimated via a simple procedure involving the solution of a linear problem and a limited set of voltage and current measurements. The above interpretation of a switching device is used to predict the CE generated by a real boost converter connected to the supply main via standard simulation tools for the frequency-domain analysis. The proposed solution, that is compared with a classical state-of-the-art LTI Norton equivalent, offers improved accuracy for different working conditions.

REFERENCES

- [1] V. Tarateeraseth, S. Kye Yak, F.G. Canavero, R.W. Chang, "Systematic Electromagnetic Interference Filter Design Based on Information From In-Circuit Impedance Measurements", *IEEE Trans. on Electromagnetic Compatibility*, Vol. 52, No. 3, pp. 588–598, Aug. 2010.
- [2] E. Rondon-Pinilla, F. Morel, C. Vollaie, J.-L. Schanen, "Modeling of a Buck Converter With a SiC JFET to Predict EMC Conducted Emissions", *IEEE Trans. on Power Electronics*, Vol. 29, No. 5, pp. 2246–2260, May 2014.

- [3] V. Tarateeraseth, I.A. Maio, F.G. Canavero, "Assessment of Equivalent Noise Source Approach for EMI Simulations of Boost Converter", *Proc. of the 20th Int. Zurich Symposium on EMC*, pp. 353–356, Jan. 2009.
- [4] Y. Liu, Kye Yak See; King-Jet Tseng, "Conducted EMI Prediction of the PFC Converter Including Nonlinear Behavior of Boost Inductor", *IEEE Trans. on EMC*, Vol. 55, No. 6, pp. 1107–1114, Dec. 2013.
- [5] F. Yang, X. Ruan, Q. Ji; Z. Ye, "Input Differential-Mode EMI of CRM Boost PFC Converter", *IEEE Trans. on Power Electronics*, Vol. 28, No. 3, pp. 1177–1188, March 2013.
- [6] R. Kahoul, Y. Azzouz, P. Marchal, B. Mazari, "New Behavioral Modeling for DC Motor Armatures Applied to Automotive EMC Characterization", *IEEE Trans on EMC*, Vol. 52, No. 4, pp. 888–901, Nov. 2010.
- [7] H. Bishnoi, A. C. Baisden, P. Mattavelli, D. Boroyevich, "Analysis of EMI Terminal Modeling of Switched Power Converters", *IEEE Trans. on Power Electronics*, Vol. 27, No. 9, pp. 3924–3933, Sept. 2012.
- [8] L. A. Zadeh, "Frequency Analysis of Variable Networks", *Proceedings of the IRE*, Vol. 38, No. 3, pp. 291–299, Mar. 1950.
- [9] R. Trinchero, I. S. Stievano, F. G. Canavero, "Steady-State Analysis of Switching Power Converters Via Augmented Time-Invariant Equivalents", *IEEE Trans. on Power Electronics*, Vol. 29, No. 11, pp. 5657–5661, Nov. 2014.
- [10] R. Trinchero, I. S. Stievano, F. G. Canavero, "EMI Prediction of Switching Converters," *IEEE Trans on EMC* (in press).
- [11] R. Trinchero, I. S. Stievano, and F. G. Canavero, "Steady-state response of periodically switched linear circuits via augmented time-invariant nodal analysis," *J. Elect. Comput. Eng.*, vol. 2014, article ID 198273, 2014.